Quadratic Pulse Inversion Ultrasonic Imaging (QPI): Detection of Low-level Harmonic Activity of Microbubble Contrast Agents

Mamoun F. Al-Mistarihi and Emad S. Ebbini
Department of Electrical and Computer Engineering, University of Minnesota, Minneapolis, MN 55455
{mamoun, emad @ece.umn.edu}

ABSTRACT

We present an ultrasonic imaging approach that combines harmonic-sensitive pulse sequences with a post-beamforming quadratic kernel derived from a second-order Volterra filter (SOVF). This approach is designed to produce images with high sensitivity to nonlinear oscillations (20 – 30 dB below the fundamental) from microbubble ultrasound contrast agents (UCA) while maintaining high levels of noise rejection. In this paper, we demonstrate the performance of this approach with pulse-inversion imaging sequence consisting of two transmit pulses with opposite polarity whose echoes are summed to enhance the even harmonics and suppress the fundamental. This is followed by an optimally designed SOVF-based quadratic kernel for further enhancing the harmonic signals, while maximizing the noise rejection. The approach is demonstrated experimentally using images from *in vivo* kidney after bolus injection with UCA. Imaging results as well as the spectral contents of QPI data show a significant increase in harmonic sensitivity and reduction in noise levels. Implications of this approach on new forms of functional ultrasound imaging are discussed.

1. INTRODUCTION

Microbubble ultrasound contrast agents (UCA) are being investigated for use in clinical imaging applications for tissue function and for targeted therapeutic applications. The objective is to detect minute concentrations of UCA in the microvasculature during ultrasonic exams thus providing a view of the perfusion in the tissue. This functional form of ultrasonic imaging is seen an important component for the continued use of ultrasound as a medical imaging modality. For example, many tumors without distinguishing characteristics on conventional ultrasound have characteristic blood perfusion patterns that allow for easy detection if a perfusion sensitive imaging is available.

Interaction between microbubbles UCAs and acoustic wave result in nonlinear harmonic echo generation. This phenomenon can be exploited to enhance the echoes from the microbubbles and, therefore, reject fundamental components resulting largely from tissue. Imaging techniques based on nonlinear oscillations have been designed for separating and enhancing nonlinear UCA echoes from a specified region of interest within the imaging field, including second harmonic (SH) B-mode imaging and pulse inversion (PI) Doppler imaging [5]. The SH imaging employs a fundamental frequency transmit pulse and produces images from the second harmonic component of received echoes by using a second harmonic bandpass filter (BPF) to remove the fundamental frequency. In order to increase UCA detection sensitivity in the limited transducer bandwidth condition, spectral overlap between fundamental and second harmonic parts need to be minimized by transmitting narrow-band pulses resulting in an inherent tradeoff between contrast and spatial resolution. In PI imaging a sequence of two inverted acoustic pulses with appropriate delay is transmitted into tissue. Images are produced by summing the corresponding two backscattered signals. In the absence of tissue motion, the resulting sum can be shown to contain only even harmonics of the nonlinear echoes. The PI imaging overcomes the tradeoff between contrast and spatial resolution because it utilizes the entire bandwidth of the backscattered signals. As a result, superior spatial resolution can be achieved when compared with SH imaging. However, the subtraction process results in significant reduction of signal to noise as the harmonics are typically 20 - 30 dB or more below the (cancelled) fundamental component.

We have previously shown that the SOVF-based quadratic kernels provide high sensitivity to harmonic echoes comparable to PI with a significant increase in dynamic range due to inherent noise rejection of quadratic filtering [6]. An algorithm for deriving the coefficients of the kernel using singular values decomposition (SVD) of a linear and quadratic prediction data matrix was proposed and experimentally validated in [7]. Imaging results and comparisons with SH and PI images have shown that quadratic imaging is superior to SH and compares favorably with PI without the need for multiple transmissions. However, due to reliance on linear and quadratic prediction, the quadratic kernel has sensitivity to the fundamental that limits its ability to detect UCA in the microvasculature.

This paper combines PI and quadratic imaging to mitigate the limitations of both methods. The approach is based on quadratic filtering of PI data that, while noisy, is largely free of fundamental tissue components. The efficiency of the quadratic kernel in rejecting noise while maintaining quadratic signal components allows the recovery of quadratic components below the noise floor. This new quadratic PI (QPI) imaging approach offers the promise of detecting

harmonic oscillations at or below the noise floor. Given the current trend of imaging UCA with extremely low transmit pulse amplitudes (to minimize nonlinear echo generation from tissue), the ability of QPI to detect quadratic signal activity below the noise floor becomes essential to the detection of harmonic activity in the 40 – 50 dB range below the fundamental. The imaging results given in this paper indicate that a signal processing approach to this clinical challenge is feasible.

2. THEORY

The algorithm in this section is based on [6-7], which have shown the validity of a SOVF as a model for pulse-echo ultrasound data from tissue mimicking media. The response of a quadratically nonlinear system with memory $\hat{y}(n+1)$, can be predicted by a second order Volterra model of *m* past values as follows:

$$\hat{y}(n+1) = \sum_{i=0}^{m-1} y(n-i)h_L(i) + \sum_{j=0}^{m-1}\sum_{k=j}^{m-1} y(n-j)y(n-k)h_Q(j,k) \quad (1)$$

where $h_L(i)$ and $h_Q(j,k)$ are the linear and quadratic filter coefficients, respectively. Using a segment of the RF data, a system of linear equations are formed and solved for elements of the quadratic kernel. Details of the algorithm to determine the quadratic kernel that provide maximum contrast enhancement have been described in [6-7].

In this paper, we present a new algorithm of post beamforming second order Volterra filter on a pulse Inversion data (QPI) to combine the features of the two techniques, improve the contrast specificity, reduce the noise component in the tissue region and recover part of the tissue component which is completely cancelled in PI image. The quadratic image is produced by applying the quadratic filter coefficients to the beamformed RF data throughout the standard B-mode and PI images to estimate the quadratic component

$$\hat{y}_Q(n+1) = \sum_{j=0}^{P-1}\sum_{k=j}^{P-1} y(n-j)y(n-k)Q(j,k) \quad (2)$$

where Q represents the quadratic kernel resulting from twice 2D autocorrelation of the quadratic kernel and P is equal to $4m$-3.

3. MATERIALS AND METHODS

3.1 Experimental setup

We evaluated the algorithm with RF data acquired from experiments conducted *in vivo* on a juvenile pig. Bolus injections of SonoVue™ (Bracco Research SA, Geneva, Switzerland), an UCA consisting of sulphur hexafluoride gas bubbles coated by a flexible phospholipidic shell, were administered with two different concentrations (0.01 mL/kg and 0.0025 mL/kg).

Three- and four-cycle pulses at 1.56 MHz were transmitted using a convex array probe (CA430E) with mechanical indices (MIs) of 0.158 and 0.152, respectively, to scan a kidney. Technos MPX ultrasound system (ESAOTE S.p.A, Genova, Italy) was modified so that a pair of inverted pulses with the appropriate time delay was subsequently transmitted to produce images with the PI technique. In addition, in order to remove low frequency components due to tissue motion artifacts and retain harmonic frequency components from UCAs, RF data from PI imaging were filtered using the linear highpass filter with cutoff frequency 2.3 MHz. For each setup, three frames of RF data from the PI technique were collected with 10 s and 15 s delays after the injection of 0.01 mL/kg and 0.0025 mL/kg UCAs, respectively. RF data were acquired with 16-bit resolution at 20-MHz sampling frequency without TGC compensation and saved for off-line processing.

3.2 Contrast measurements

As a comparison of contrast enhancement between images from different techniques, we determine CTRs from data in the RF domain before scan converted. CTRs of images can be calculated with echoes from two referenced regions: First, the contrast region inside the kidney (bottom-left part). Second, the tissue region outside the kidney (on the left hand side of the contrast region with the same depth). Both regions are composed of 21 connected A-lines with 7.5-mm axial extent.

4. RESULTS AND DISCUSSION

Fig. 1 shows images obtained using a standard B-mode image of the kidney after the injection of 0.01 mL/kg UCAs acquired using 3-cycle transmission, PI, second harmonic on PI data (SHPI), quadratic image from twice 2D correlation of 38th singular mode of the B-mode data, and quadratic image from twice 2D correlation of the 2nd singular mode of the PI data. Due to differences in dynamic ranges, each image is displayed with its full dynamic range as can be seen from the dB-level scale bars. Due to low microbubble populations in the perfused tissue of the kidney (Standard B-mode image), echogenicity from contrast regions is slightly lower than that from surrounding tissue regions, which agrees with the CTR value (-2.1175 dB) whereas the PI image provides CTR 14.3630 dB, echogenicity of the contrast region from the PI image appears brighter than that from surrounding tissue regions. Please note that the CTR value for the PI image without SH filtering was only 10.2319 dB, i.e. there is a 4.1311 dB gain due to the removal of tissue components introduced by motion. It is also worth noting that the SH image on the B-mode data suffers from significant loss in spatial resolution. The quadratic image from twice 2D correlation of 38th singular mode provides CTR 23.1298 dB,

which shows a contrast enhancement over both standard B-mode, PI and SHPI images.

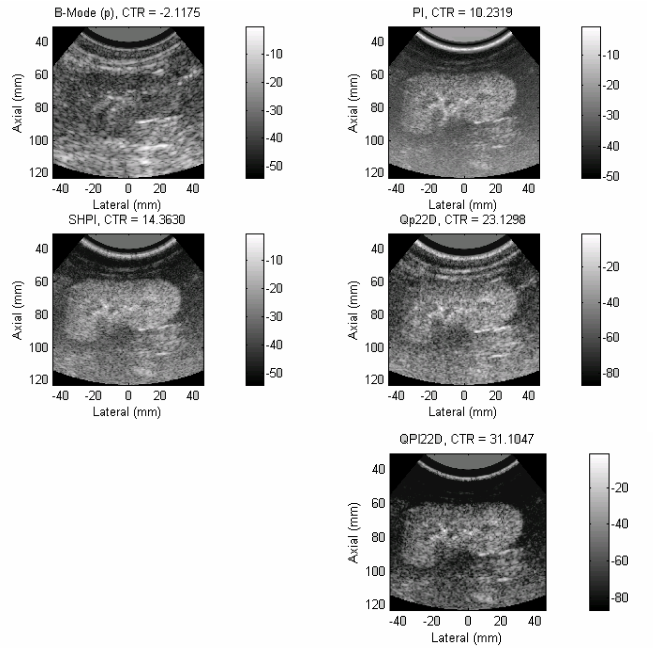

Fig. 1 Images of the: Standard B-mode image of the kidney at 10 s after the injection of 0.01 mL/kg, PI, SHPI, quadratic from twice 2D correlation of 38th singular mode of the B-mode data, and quadratic from twice 2D correlation of the 2nd singular mode of the PI data (QPI).

The quadratic image from twice 2D correlation of the 2nd singular mode of the PI data (QPI) is obtained using the algorithm described in section 2 with the use of a 5.6-mm contrast A-line and a system order 15, provides CTR 31.1047 dB, which shows a contrast enhancement over the other four images. We can clearly see not only the kidney's shape and boundary due to UCA echoes but also large vascular structures as it is seen in the PI, SHPI, quadratic from twice 2D correlation of 38th singular mode images too. Also we can see that the kidney's shape and boundary due to UCA echoes are the clearest in the QPI image compared with the other four images due to reduction of the noise component in the tissue region and recovering part of the tissue component which is completely cancelled in the PI image.

Fig. 2 shows the average spectra of data from the UCA and tissue region produced from the images shown in Fig. 1 where the UCA spectra are shown in dark solid line while the tissue spectra are shown in lighter solid line.

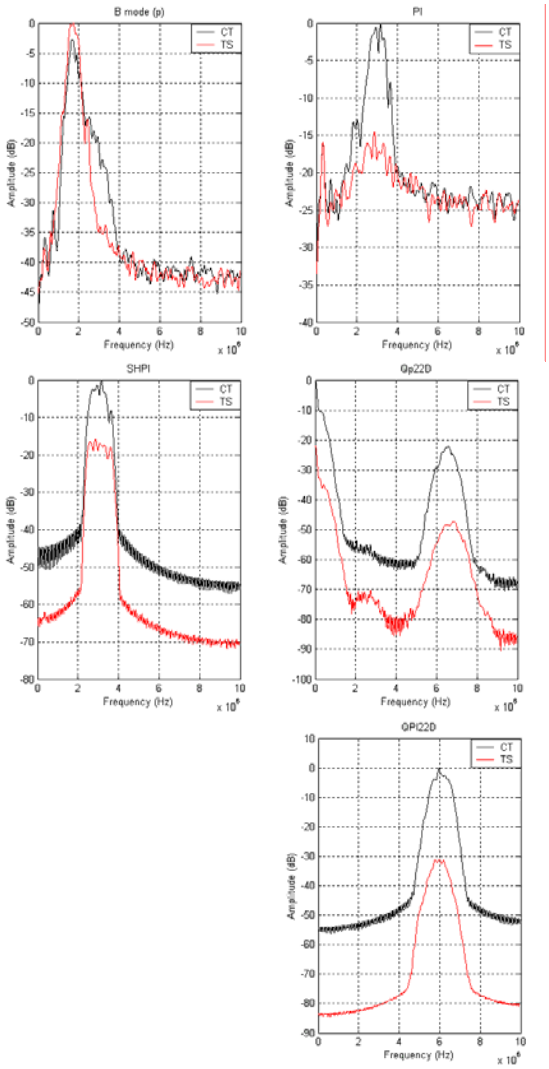

Fig. 2 Average spectra from the contrast (darker) and tissue (lighter) of the kidney: Standard B-mode, PI, SHPI, quadratic from twice 2D correlation of 38th singular mode of the B-mode data, and quadratic from twice 2D correlation of the 2nd singular mode of the PI data.

The spectra of the B-mode image shows spectral peaks at the fundamental and 2nd harmonic. It is interesting to see that the PI data and the SHPI data show spectral peaks at the 2nd harmonic whereas the quadratic components show spectral peaks at low-frequency and at 6.6 MHz which is twice the 2nd harmonic of the B-mode image. In addition, spectra from the QPI image shows a spectral peak at twice the 2nd harmonic of the B-mode image. The spectra of the PI, SHPI, quadratic from twice 2D correlation of 38th singular mode of the B-mode data and QPI images deal with the 2nd harmonic of the B-mode image as a fundamental frequency. Also from the spectra of the QPI, the noise component in the tissue region is reduced and the QPI algorithm recovers part of the tissue component.

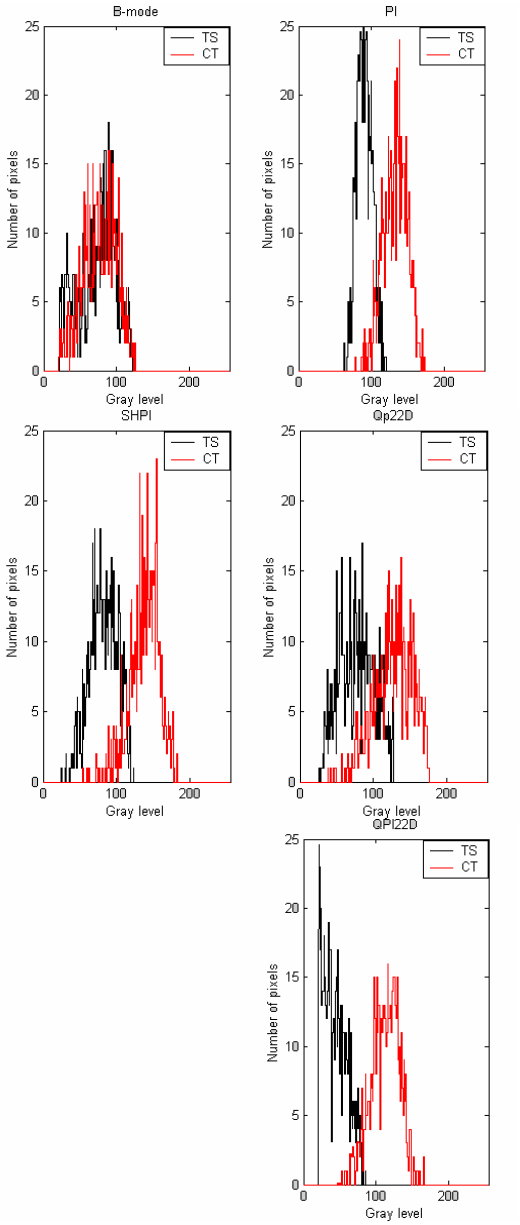

Fig. 3 Gray-level histograms produced from images shown in Fig. 1. Histograms are produced from the contrast region (lighter) and the tissue region (darker).

Fig. 3 shows the gray-level histograms produced from the standard B-mode, PI, SHPI, quadratic from twice 2D correlation of 38th singular mode of the B-mode data, and quadratic from twice 2D correlation of the 2nd singular mode of the PI data images. In each case, the histogram from the UCA region is plotted with light solid line, while the histogram from tissue is plotted with darker solid line. One can see the degree of overlap between the histograms is highest for the standard B-mode image, whereas it is the lowest for the QPI image.

5. CONCLUSIONS

The results shown in this paper indicate clearly that QPI imaging is far superior to either PI or quadratic imaging alone. This is due to the fact that applying quadratic filtering to Pulse-inversion data (in that order) allows the cascade to efficiently mitigate the limitations of either imaging method applied alone. Specifically, PI processing efficiently removes fundamental tissue components, but amplifies the noise floor thus masking low-level harmonic activity. The quadratic kernel can be designed to efficiently remove noise throughout the spectrum while maintaining quadratic data, even below the noise floor, which is not possible with linear filters. On the other hand, the ability of PI processing to eliminate fundamental tissue components is essential because the quadratic kernel derived from a prediction model is often sensitive to correlated fundamental data. Both CTR values and spectral contents of QPI data compared to PI, SHPI, and Q data alone demonstrate the improved performance of this new approach.

6. REFERENCES

[1] K. I. Kim and E. J. Powers, "A digital method of modeling quadratically nonlinear systems with a general random input," *IEEE Trans. Acoust., Speech, Signal Processing,* vol. 36, no. 11, pp. 1758-1769, Nov. 1988.

[2] T. Koh and E. J. Powers, "Second-order volterra filtering and its application to nonlinear system identification," *IEEE Trans. Acoust., Speech, Signal Processing,* vol. ASSP-33, no. 6, pp. 1445-1455, Dec. 1985.

[3] H. Yao, P. Phukpattaranont, and E. S. Ebbini, "Post-beamforming second-order Volterra filter for nonlinear pulse-echo imaging," *ICASSP,* pp. 1133-1136, 2002.

[4] J. Ophir and K. J. Parker, "Contrast agent in diagnostic ultrasound," *Ultrasound in Med. & Biol.,* vol. 15, no. 4, pp. 319-333, Nov. 1989.

[5] D. H. Simpson, C. T. Chin, and P. N. Burns, "Pulse inversion Doppler: A new method for detecting nonlinear echoes from microbubble contrast agent," *IEEE Trans. Ultrason., Ferroelect., Freq. Contr.,* vol. 46, no. 2, pp. 372-382, Mar. 1999.

[6] P. Phukpattaranont and E. S. Ebbini, "Post-beamforming second-order Volterra filter for nonlinear pulse-echo ultrasonic imaging," *IEEE Trans. Ultrason., Ferroelect., Freg. Contr*., vol. 50, no. 8, pp. 987-1001, Aug. 2003.

[7] P. Phukpattaranont, M. F. Al-Mistarihi and E. S. Ebbini, 'Post-beamforming Volterra filters for contrast-assisted ultrasonic imaging: In-vivo results," in *Proc. IEEE Ultrason. Symp*., 2003.

[8] M. F. Al-Mistarihi, P. Phukpattaranont and E. S. Ebbini, "A Two-Step Procedure For Optimization Of Contrast Sensitivity And Specificity Of Post-Beamforming Volterra Filters" in *Proc. IEEE UFFC* 2004.